18th International Conference
ENGINEERING MECHANICS 2012
Svratka, Czech Republic, May 14 – 17, 2012

pp. 5–21
Paper #97

TWO-SCALE MODELLING OF STRONGLY HETEROGENEOUS CONTINUA USING THE HOMOGENIZATION APPROACH

E. Rohan* **R. Cimrman**** **V. Lukeš*****

Abstract: *The notion of strong heterogeneity is considered in the sense of material scaling: the idea is to study mathematical models where the coefficients of the partial differential equations associated with one of the material phases depend on the characteristic size ε of the microstructure. This modeling ansatz is justified to represent high contrasts in material properties of different components; it was applied to study wave propagation in two-phase elastic composites with "weak" inclusions, where elasticity is scaled by ε^2, or to describe poroelastic behaviour in double-porous media, where permeability of the second porosity is proportional ε^2. Perforated structures can be handled using similar mathematical tools. For homogenization of thin structures the scaling is related to the thickness, which leads to reduced spatial dimension of the problem. This paper summarizes some models developed using the homogenization approach; namely applications in modelling elastic waves, acoustic transmission and fluid flow in porous media are discussed.*

Keywords: ***homogenization, composites, wave propagation, porous media, perfusion***

1. Introduction

In the context of material modeling, the notion of homogenization is related usually to some approximate treatment of heterogeneous continua designed as mixtures of different constituents. The differences concern just values of the material parameters, or they are more substantial – for instance mixtures of fluid and solid components are considered. In the mechanical community, the homogenization is often understood in the sense of various averaging techniques based on definition of the RVE, the reference volume element. The RVE (small enough, but also sufficiently large) is subject to special loadings and the structural responses allow to compute the effective parameters characterizing the material behaviour. Apart of this averaging technique, there is the Eshelby theory which can describe behaviour of composites with elliptic inclusions which do not affect each other, being sparsely distributed at long distances.

The homogenization we have in mind is based on the asymptotic analysis of partial differential equations describing the continuum behaviour, whereby the small parameter describing the "microstructure size" influences space variation of the equation coefficients. We focus on problems characterized by strong heterogeneities — *large contrasts* in material coefficients; it is shown how the large contrast pronounced by its relationship with the scale may lead to "limit behaviour" which is qualitatively completely different from the one characterizing the original constituents.

Nowadays there exist several methods which allow one to obtain a model of homogenized continuum, i.e. by studying asymptotic behaviour of partial differential equations (PDEs) which governs a given problem characterized by the scale ε. The **periodic unfolding** which has been introduced and employed within the homogenization community recently, Cioranescu et al. (2008a), is relatively easy to use for linear, or quasi-linear problems. It presents a powerful tool for homogenization of locally periodic media even for those who have merely a little training in functional analysis.

Challenges and limitations. The asymptotic analysis of heterogeneous media provides a modeling tool which enables to retain important features of the structure (or microstructure) while reducing complexity of the problem in its primary setting. Periodically distributed structural details inducing some

* Prof. Dr. Ing. Eduard Rohan: Faculty of Applied Sciences, University of West Bohemia in Pilsen, Univerzitní 22, 306 14 Plzeň; CZ, e-mail: rohan@kme.zcu.cz
** Ing. Robert Cimrman, Ph.D.: New Technologies Research Centre, University of West Bohemia in Pilsen, Univerzitní 22, 306 14 Plzeň; CZ, e-mail: cimrman3@ntc.zcu.cz
*** Ing. Vladimír Lukeš, Ph.D.: Faculty of Applied Sciences, University of West Bohemia in Pilsen, Univerzitní 22, 306 14 Plzeň; CZ, e-mail: lukes@kme.zcu.cz

fluctuations of the physical fields can be condensed into the homogenized coefficients of the limit macroscopic (i.e. homogenized) model. Its numerical discretization leads to a computationally tractable problem which can be solved much cheaper than the original problem discretized with enormously large numbers of degrees of freedom, such that a huge computational power would be required to obtain a solution. Obviously, the benefits of "simplified" models obtained by homogenization is even more challenging when inverse problems are treated, like optimal design of the material structure.

However, the homogenized models describe the asymptotic behaviour, so that the limit behaviour is just an approximation of the reality which corresponds to a given scale $\varepsilon_0 > 0$. Apparently, the approximation becomes more accurate with decreasing ε_0, i.e. when the macroscopic structure involves more and more repeating microstructural periods.

Once the global response is known, having solved the macroscopic problem, the detail fluctuating response at the microscopic level can be computed for a given macroscopic position x. This procedure is often called the *microscopic response recovery* and is based on the *corrector functions*. They are obtained by combining the macroscopic solution at x with the local *corrector basis functions*. Thus, also the gradients of the quantity of interest can be obtained, like strains, stresses, or seepage velocities in porous media.

Models with scale-dependent parameters, like models of large contrast composites as an example, may amplify some special effects when passing to the limit with $\varepsilon \to 0$. For instance, limit model of the high contrast elasticity medium exhibits the dispersive behaviour, although the standard composites lead to a nondispersive medium which, in the limit, is characterized by the homogenized elasticity and by the mean-value of the density. In contrast, the ε^2-scaling of the elasticity coefficients in one of the composite constituents results in a frequency-dependent homogenized mass coefficients, hence the wave dispersion is obtained even in the limit $\varepsilon \to 0$.

It is worth to note that the standard homogenized model of composites preserve the homogeneous medium when all the constituents are identical, i.e. homogenization of a homogeneous material results in the same material. This is not possible, in principle, for a heterogeneous medium with scale-dependent parameters which, providing a strong heterogeneity, does not allow to obtain any standard homogeneous medium in the limit.

The main issues discussed in the paper are the following:

- **Homogenization applied in wave propagation problems**. Only solid composite materials are considered here, although an extension for fluid saturated media has been addressed by Mielke and Rohan (2012). The main focus is in the phononic materials ("band-gap materials"), characterized by large heterogeneity in the elasticity coefficients, and in the acoustic transmission on perforated interfaces immersed in the acoustic fluid. Extensions to electromagnetic waves and piezoelectric composites were treated also Leugering et al. (2010).
- **Homogenization of fluid-saturated porous materials** (FSPM) with *double porosity*. It is shown how different topologies of the microstructure with respect to double porosity lead to qualitatively different models. An extension for large-deforming media was proposed, which is based on linearized subproblems. Finally, homogenization of the *fluid perfusion in layered double-porous medium* is described. These topics have applications in modeling the tissue perfusion and in modeling bone poroelasticity.

2. Wave propagation and dispersion in heterogeneous media

In the context of the homogenization method, waves in solid composites and solid-fluid mixtures have been discussed e.g. in Sanchez-Palencia (1980). The classical treatment of elastic waves leads to vanishing wave dispersion in the limit $\varepsilon \to 0$, however, the approach reported by Ávila et al. (2008); Rohan et al. (2009); Rohan and Miara (2009, 2011) allows to retain the dispersion properties even in the limit; this is possible due to the *strong heterogeneity* – large contrast in the elasticity coefficients and the special scaling ansatz of these coefficients. Besides the elastic composites, some other topics related to wave propagation were considered, namely those related to piezo-materials and acoustic waves on a perforated interface.

Combinations of all these topics are natural and challenging in the view of modeling smart systems transmitting waves:

- *Piezo-phononic materials* form a quite natural extension of the purely elastic phononic materials, they provide even more flexibility in designing smart devices, due to possible interplay between the electric field and deformations. The homogenization issues were discussed in Rohan and Miara (2006b, 2009); Cimrman and Rohan (2010).
- It is desirable to extend the acoustic transmission conditions for *compliant perforated plates*, when the plate elasticity cannot be neglected. Moreover, the surface acoustic waves propagating along the interface may interfere with the plate structure – the plate can be constructed as a phononic, or piezo-phononic material, so that band gaps of the plate can influence qualitatively the acoustic transmission in the surrounding medium.
- For homogenization of the electromagnetic waves, analogical methods and modeling approaches are applied, as those introduced in the study of elastic waves. Moreover, in combination with piezoelectric materials, coupling between acoustic and electromagnetic waves is a relevant issue.

2.1. Phononic materials

The *phononic materials (crystals)* are multi-phasic (bi-phasic) elastic media with periodic structure and with large contrasts in elasticity of the phases. Often they are called the *phononic band-gap materials* due to their essential property to suppress propagation of elastic waves in certain frequency ranges. The phononic crystals are used in modern technologies to generate frequency filters, beam splitters, sound or vibration protection devices (for noise reduction), or they may serve as waveguides. Similar phenomena in the propagation of the electromagnetic field were studied even before in the context of the *photonic crystals*.

The method of homogenization provides a useful modeling tool which allows for prediction of the band gap distribution for stationary or long guided waves. The "standard computational approach" based on a full heterogeneous model requires to evaluate the whole Brillouin zone for the dispersion diagram reconstruction; as the consequence, it leads to a killing computational complexity. On the other hand, the homogenized model captures the essential features of the phononic material and may serve a good approximation of the band-gap prediction, while keeping the computational complexity at a very low level. As an advantage, the homogenized model can be employed in inverse problems like optimal design of phononic structures.

Periodic strongly heterogeneous material We consider an open bounded domain $\Omega \subset \mathbb{R}^3$ and the reference (unit) cell $Y =]0,1[^3$ with an embedded inclusion $\overline{Y_2} \subset Y$, whereby the matrix part is $Y_1 = Y \setminus \overline{Y_2}$. Let us note, that Y may be defined more generally as a parallelepiped. Using the reference cell we generate the decomposition of Ω into the union of inclusions and the matrix. Inclusions have the size $\sim \varepsilon$,

$$\Omega_2^\varepsilon = inter \bigcup_{k\in\mathbb{K}^\varepsilon} \varepsilon(\overline{Y_2}+k)\ , \text{ where } \mathbb{K}^\varepsilon = \{k\in\mathbb{Z}|\ \varepsilon(k+\overline{Y_2})\subset\Omega\}\ , \tag{1}$$

whereas the perforated matrix is $\Omega_1^\varepsilon = \Omega \setminus \overline{\Omega_2^\varepsilon}$.

We assume that inclusions are occupied by a "very soft material" in the sense that the coefficients of *the elasticity tensor in the inclusions* are significantly smaller than those of the matrix compartment, however *the material density* is comparable in both the compartments. Such structures exhibit remarkable band gaps; this was proved by both experiments and modeling. Here, as an important feature of the modeling based on asymptotic analysis, the ε^2 scaling of elasticity coefficients in the inclusions appears; the following ansatz is considered:

$$\rho^\varepsilon(x) = \begin{cases} \rho^1 & \text{in } \Omega_1^\varepsilon, \\ \rho^2 & \text{in } \Omega_2^\varepsilon, \end{cases} \qquad c_{ijkl}^\varepsilon(x) = \begin{cases} c_{ijkl}^1 & \text{in } \Omega_1^\varepsilon, \\ \varepsilon^2 c_{ijkl}^2 & \text{in } \Omega_2^\varepsilon. \end{cases} \tag{2}$$

In analogy, the PZ phononic materials can be treated.

Modeling the stationary waves We consider stationary wave propagation in the medium introduced above. Although the problem can be treated for a general case of boundary conditions, for simplicity we restrict the model to the description of clamped structures loaded by volume forces. We assume harmonic single-frequency volume forces $\boldsymbol{F}(x,t) = \boldsymbol{f}(x)e^{i\omega t}$, where $\boldsymbol{f} = (f_i), i = 1,2,3$ is its local amplitude and ω is the frequency. Correspondingly, a dispersive displacement field with the local magnitude $\boldsymbol{u}^\varepsilon$ has the form $\boldsymbol{U}^\varepsilon(x,\omega,t) = \boldsymbol{u}^\varepsilon(x,\omega)e^{i\omega t}$. This allows us to study the steady periodic response of the medium, as characterized by displacement field $\boldsymbol{u}^\varepsilon$ which satisfies the following boundary value problem:

$$\begin{aligned} -\omega^2\rho^\varepsilon\boldsymbol{u}^\varepsilon - \mathrm{div}\boldsymbol{\sigma}^\varepsilon = \rho^\varepsilon\boldsymbol{f} \quad \text{in } \Omega, \\ \boldsymbol{u}^\varepsilon = 0 \quad \text{on } \partial\Omega, \end{aligned} \tag{3}$$

where the stress tensor $\boldsymbol{\sigma}^\varepsilon = (\sigma_{ij}^\varepsilon)$ is expressed in terms of the linearized strain tensor $\boldsymbol{e}^\varepsilon = (e_{ij}^\varepsilon)$ by the Hooke's law $\sigma_{ij}^\varepsilon = c_{ijkl}^\varepsilon e_{kl}(\boldsymbol{u}^\varepsilon)$.

Homogenized model Due to the *strong heterogeneity* in the elastic coefficients, the homogenized model exhibits dispersive behaviour; this phenomenon cannot be observed when standard two-scale homogenization procedure is applied to a medium without scale-dependent material parameters. In Ávila et al. (2008) the unfolding operator method of homogenization (Cioranescu et al., 2008a) was applied with the strong heterogeneity ansatz (2) and in Rohan and Miara (2006b) the analogous result was obtained for the piezoelectric material with the strong heterogeneity scaling.

The resulting limit equations, as derived in Ávila et al. (2008), describe the structure behaviour at the "macroscopic"scale. They involve the homogenized coefficients which depend on the characteristic responses at the "microscopic" scale.

The frequency–dependent homogenized mass involved in the macroscopic momentum equation is expressed in terms of eigenelements $(\lambda^r, \boldsymbol{\varphi}^r) \in \mathbb{R}\times\mathbf{H}_0^1(Y_2), r = 1,2,\ldots$ of the elastic spectral problem which is imposed in inclusion Y_2 with $\boldsymbol{\varphi}^r = 0$ on ∂Y_2:

$$\int_{Y_2} c_{ijkl}^2 e_{kl}^y(\boldsymbol{\varphi}^r)\, e_{ij}^y(\boldsymbol{v}) = \lambda^r \int_{Y_2} \rho^2\boldsymbol{\varphi}^r\cdot\boldsymbol{v} \quad \forall\boldsymbol{v}\in\mathbf{H}_0^1(Y_2)\ , \quad \int_{Y_2}\rho^2\boldsymbol{\varphi}^r\cdot\boldsymbol{\varphi}^s = \delta_{rs}\ . \tag{4}$$

To simplify the notation we introduce the *eigenmomentum* $\boldsymbol{m}^r = (m_i^r)$,

$$\boldsymbol{m}^r = \int_{Y_2}\rho^2\boldsymbol{\varphi}^r. \tag{5}$$

The effective mass of the homogenized medium is represented by mass tensor $\boldsymbol{M}^* = (M_{ij}^*)$, which is evaluated as

$$M_{ij}^*(\omega^2) = \frac{1}{|Y|}\int_Y \rho\delta_{ij} - \frac{1}{|Y|}\sum_{r\geq 1}\frac{\omega^2}{\omega^2-\lambda^r} m_i^r m_j^r\ ; \tag{6}$$

The elasticity coefficients are computed just using the same formula as for the perforated matrix domain, thus being independent of the material in inclusions:

$$C_{ijkl}^* = \frac{1}{|Y|}\int_{Y_1} c_{pqrs}e_{rs}^y(\boldsymbol{w}^{kl}+\boldsymbol{\Pi}^{kl})e_{pq}(\boldsymbol{w}^{ij}+\boldsymbol{\Pi}^{ij})\ , \tag{7}$$

where $\boldsymbol{\Pi}^{kl} = (\Pi_i^{kl}) = (y_l\delta_{ik})$ and $\boldsymbol{w}^{kl}\in\mathbf{H}_\#^1(Y_1)$ are the corrector functions satisfying

$$\int_{Y_1} c_{pqrs}e_{rs}^y(\boldsymbol{w}^{kl}+\boldsymbol{\Pi}^{kl})e_{pq}^y(\boldsymbol{v}) = 0 \quad \forall\boldsymbol{v}\in\mathbf{H}_\#^1(Y_1)\ . \tag{8}$$

Above $\mathbf{H}_\#^1(Y_1)$ is the restriction of $\mathbf{H}^1(Y_1)$ to the Y-periodic functions (periodicity w.r.t. the homologous points on the opposit edges of ∂Y).

The *homogenized equation* of the "macromodel", here presented in its differential form, describes the macroscopic displacement field $\boldsymbol{u}$:

$$\omega^2 M^*_{ij}(\omega) u_j + \frac{\partial}{\partial x_j} C^*_{ijkl} e_{kl}(\boldsymbol{u}) = M^*_{ij}(\omega) f_j \ , \tag{9}$$

where M^*_{ij} at the r.h.s. loading term appears due to the volume forces in (3) proportional to the density.

Using this equation, the dispersion of guided waves can be studied, see Rohan et al. (2009). Heterogeneous structures with finite scale of heterogeneities exhibit the frequency *band gaps* for certain frequency bands. In the *homogeneized medium*, waves can be propagated provided the mass tensor $\boldsymbol{M}^*(\omega)$ is positive definite, or positive semidefinite; this effect is explained below.

We can derive a homogenized model analogous to (9) also for the *piezoelectric phononic* (piezophononic) materials with "soft inclusions", i.e. the scaling (2) is adopted also for parameters of dielectricity, d_{ij}, and piezoelectric coupling, g_{kij}. In this case, however, the spectral problem analogous to (4) comprises an additional constraint arising from electric charge conservation, see Rohan and Miara (2006b); Cimrman and Rohan (2010) for details.

Band gap prediction As the main advantage of the homogenized model (9), by analyzing the dependence $\omega \to \boldsymbol{M}^*(\omega)$ one can determine distribution of the band gaps; it was proved in Ávila et al. (2008), *cf.* Rohan et al. (2009) that there exist frequency intervals G^k, $k = 1, 2, \ldots$ such that for $\omega \in G^k \subset]\lambda^k, \lambda^{k+1}[$ at least one eigenvalue of tensor $M^*_{ij}(\omega)$ is negative. Those intervals where all eigenvalues γ_M of M^*_{ij} are negative are called *strong*, or *full* band gaps. In the latter case the negative sign of the mass changes the hyperbolic type of the wave equation to the elliptic one, therefore, no waves can propagate. In the "weak" bad gap situation only waves with certain polarization can propagate, as explained below.

The band gaps can be classified w.r.t. the waves polarization which is determined in terms of the eigenvectors of $M^*_{ij}(\omega)$. Given a frequency ω, there are three cases to be distinguished according to the signs of eigenvalues $\gamma^r_M(\omega)$, $r = 1, 2, 3$ (in 3D), determining the "positivity, or negativity" of the mass:

1. **propagation zone** – All eigenvalues of $M^*_{ij}(\omega)$ are positive: then homogenized model (9) admits wave propagation without any restriction of the wave polarization;

2. **strong band gap** – All eigenvalues of $M^*_{ij}(\omega)$ are negative: then homogenized model (9) does *not* admit any wave propagation;

3. **weak band gap** – Tensor $M^*_{ij}(\omega)$ is indefinite, i.e. there is at least one negative and one positive eigenvalue: then propagation is possible only for waves polarized in a manifold determined by eigenvectors associated with positive eigenvalues. In this case the notion of wave propagation has a local character, since the "desired wave polarization" may depend locally on the position in Ω.

In Fig. 1 we introduce a graphical illustration of the band gaps analyzed for an L-shaped inclusions. If inclusions (considered in 2D) are symmetric w.r.t. more than 1 axis of symmetry, than only strong band gaps exist. More details on the band gap properties and their relationship to the dispersion of guided waves were discussed in Rohan et al. (2009).

Piezo-electric (PZ) materials. Homogenization of a standard PZ heterogeneous medium leads to the effective constitutive law of the standard form, whereby the effective material parameters are computed for a specific microstructure. However, in Rohan and Miara (2006a) we show that combination of two standard PZ materials can lead to a new material with unusual and interesting properties (new non-zero entry in the coupling tensor) — this is the key for designing the so-called metamaterials, *cf.* Rohan and Miara (2009); Leugering et al. (2010). The PZ materials with large contrasts (respected by scaling in analogy with (2)) in all PZ coefficients were considered in homogenization of *phononic materials*, see Rohan and Miara (2006b); Cimrman and Rohan (2010). It is worth noting that for HZ the above mentioned statements on the structural symmetry do not hold because of the material anisotropy; typically only the weak band gaps exist (Cimrman and Rohan, 2010).

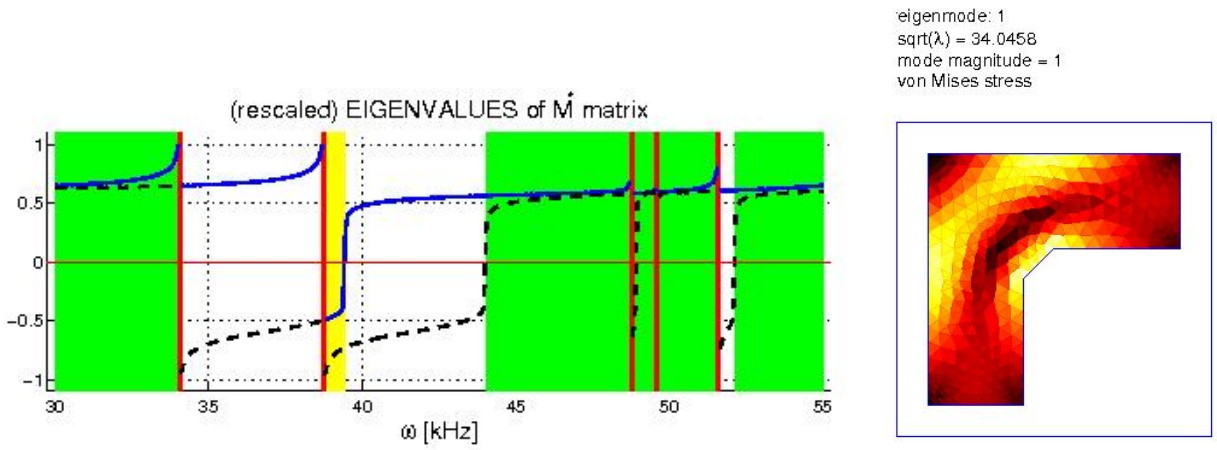

Fig. 1: Left: weak band gaps (white) and strong band gaps (yellow) computed for an elastic composite with L-shaped inclusions, the green bands are propagation zones (the solid and dashed curves describe eigenvalues of $\mathbf{M}^*(\omega)$*); Right: the first eigenmode of the L-shaped clamped elastic inclusion.*

2.2. Acoustic wave transmission on perforated interfaces

Homogenization can be employed to develop approximate models of various transmission and transport phenomena on thin interfaces characterized by a "microstructure" (Cioranescu et al., 2008b). In Rohan and Lukeš (2010b) the homogenization is applied to approximate the acoustic transmission between two halfspaces separated by an interface formed as a solid (rigid) plate perforated periodically by holes of arbitrary shapes, so that the two halfspaces are connected. We consider the acoustic medium occupying domain Ω^G which is subdivided by perforated plane Γ_0 in two disjoint subdomains Ω^+ and Ω^-, so that $\Omega^G = \Omega^+ \cup \Omega^- \cup \Gamma_0$. Denoting by p the acoustic pressure field in $\Omega^+ \cup \Omega^-$, in a case of no convection flow, the acoustic waves in Ω^G are described by the following equations (ω is the frequency of the incident wave related to wave number k through the speed of sound propagation $c = \omega/k$),

$$\begin{aligned} c^2\nabla^2 p + \omega^2 p = 0 \quad &\text{in } \Omega^- \cup \Omega^+ \,, \\ + \text{ boundary conditions} \quad &\text{on } \partial\Omega^G \,, \end{aligned} \tag{10}$$

supplemented by transmission conditions on interface Γ_0. In Rohan and Lukeš (2010b) such conditions were obtained by the two-scale homogenization of a layer with an immersed sieve-like obstacle. In Figure 2 we illustrate such a layer $\Omega_\delta = \Gamma_0 \times]-\delta/2, \delta/2[\subset \mathbb{R}^3$ embedded in $\Omega^G = \Omega^+_\delta \cup \Omega^+_\delta \cup \Omega_\delta \cup \Gamma^\pm_\delta$. The acoustic medium occupies domain $\Omega^\varepsilon_\delta = \Omega_\delta \setminus \overline{S^\varepsilon_\delta}$, where S^ε_δ is the solid *rigid* obstacle which in a simple layout has a form of the periodically perforated slab. However, the aim of the study by Rohan and Lukeš (2010b) was to obtain transmission conditions which describe quite general shape of periodic perforations.

To derive the transmission conditions, the acoustic waves in the layer were subject to asymptotic analysis w.r.t. size of the perforation ε which is related to the thickness $\delta = h\varepsilon$, where $h > 0$ is fixed. The acoustic potential $p^{\varepsilon\delta}$ satisfies the Helmholtz equation in $\Omega^\varepsilon_\delta$

$$\begin{aligned} c^2\nabla^2 p^{\varepsilon\delta} + \omega^2 p^{\varepsilon\delta} = 0 \quad &\text{in } \Omega^\varepsilon_\delta \,, \\ c^2 \frac{\partial p^{\varepsilon\delta}}{\partial n^\delta} = -\mathrm{i}\omega g^{\varepsilon\delta\pm} \quad &\text{on } \Gamma^\pm_\delta \,, \\ \frac{\partial p^{\varepsilon\delta}}{\partial n^\delta} = 0 \quad &\text{on } \partial S^\varepsilon_\delta \cup \partial\Omega^\infty_\delta \,, \end{aligned} \tag{11}$$

where by n^δ we denote the normal vector outward to Ω_δ. Assuming convergence of the interface fluxes (velocities) $g^{\varepsilon\delta} \to g^0$ (in a sence), by homogenization $\varepsilon \to 0$, convergence of $p^{\varepsilon\delta} \to p^0$ is obtained and (11) transforms into the following equations involving homogenized coefficients A, B, F and the layer

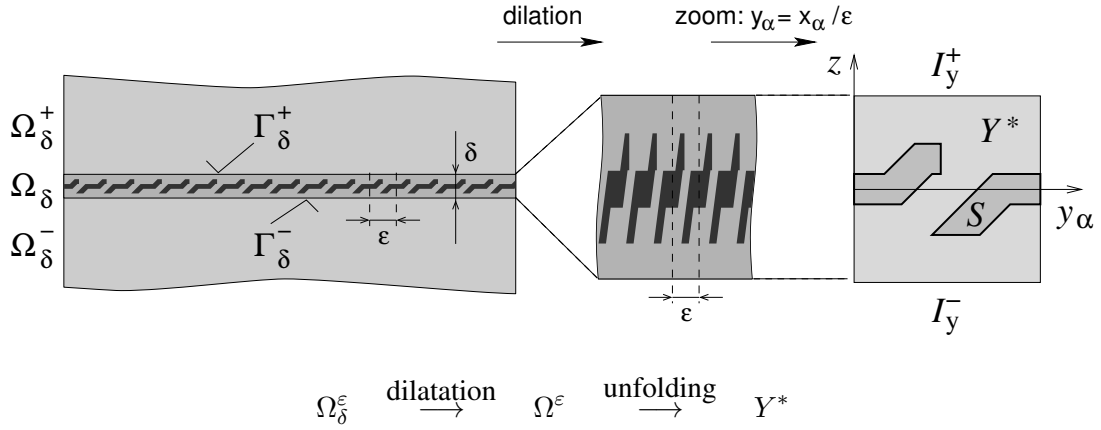

Fig. 2: Left: global problem imposed in entire domain Ω^G before homogenization of the layer Ω_δ. Right: representative cell of the periodic structure. The dark patterns represent the obstacles in the fluid.

porosity f^*,

$$\begin{aligned} -\partial_\alpha(A_{\alpha\beta}\partial_\beta p^0) + \omega^2 f^* p^0 - \mathrm{i}\omega\partial_\alpha(B_\alpha g^0) = 0 \quad &\text{on } \Gamma_0\ , \\ -\mathrm{i}\omega h B_\beta \partial_\beta p^0 + \omega^2 F g^0 = -\mathrm{i}\omega\frac{1}{\varepsilon_0}[p]_-^+ \quad &\text{on } \Gamma_0\ , \\ A_{\alpha\beta}\partial_\beta p^0 = 0 \quad &\text{on } \partial\Gamma_0\ , \end{aligned} \tag{12}$$

where $[p]_-^+/\varepsilon_0$ is the jump of p relative to the "real" layer thickness $h\varepsilon_0 > 0$ and is evaluated on Γ_0 by the acoustic potential field p in Ω^G. To compute A, B, F, microscopic problems have to be solved in the reference microscopic cell $Y^* = Y \setminus \overline{S}$, where domain S represents the obstacle generating the perforation, see Fig. 2 (right).

For the "global problem" (10), the transmission conditions are presented in an implicit form by equations (12): they couple $[p]_-^+$ with normal derivatives $\partial p/\partial n^+ = -\partial p/\partial n^- = -\mathrm{i}\omega g^0$, whereby p^0 describing the "in-layer" wave serves as an internal variable of the model. Out of resonances, p^0 vanishes when $(B_\beta) = 0$, see Fig. 3, Amic #1.

To illustrate influence of the perforation design on the global acoustic response in domain Ω^G, in Fig. 3 the transmission losses for a waveguide fitted with two different perforations on Γ_0 is depicted.

3. Fluid saturated porous media (FSPM) with dual porosity

The models of *fluid saturated porous media* (FSPM) which we have in mind are relevant to the scale where individual fluid-filled pores are not distinguishable, so that at any point of the bulk material both the solid and fluid phases are present, being distributed according to the volume fractions, cf. Coussy (2004); de Boer (2000). The phenomenological description was developed by M. Biot (Biot, 1955); his model is considered here as a basis for modeling media with large contrasts in the hydraulic permeability coefficients, thus, presenting the *strong heterogeneity*. Such a modeling option is related to the notion of the double porosity (Auriault and Boutin, 1992; Arbogast et al., 1990) which introduces yet another scale with even smaller characteristic size than the one characterizing the "microscopic level".

Two important phenomena can be noticed when homogenizing the FSPM:

- In high contrast media, in general, the topology of the microstructure decomposition influences qualitatively the homogenization result.
- When evolutionary models are homogenized, the fading memory effect of the homogenized constitutive laws arise from the fluid microflow governed by the Darcy law.

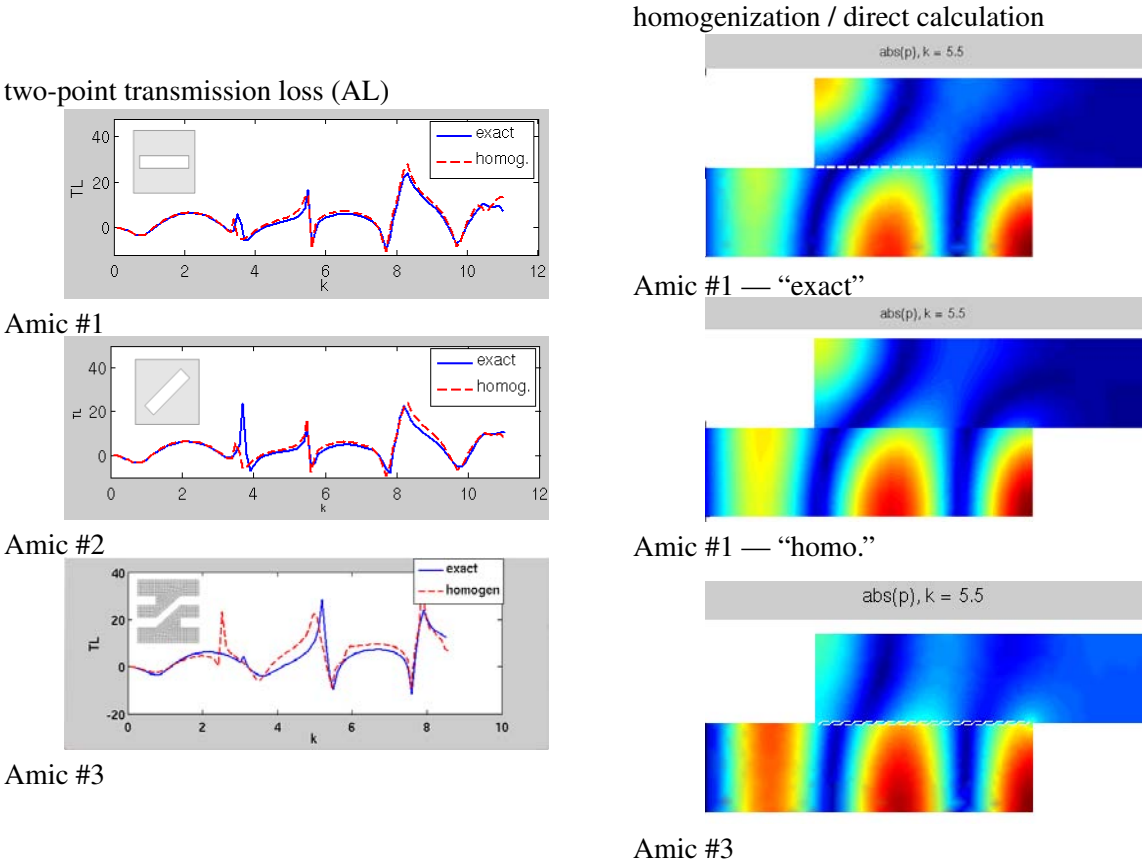

Fig. 3: Left: Transmission losses for three perforation types, #1,#2#3; comparison of solutions obtained for the homogenized transmission conditions (dashed line) with the corresponding direct approximation of the perforated domains (solid line). Right: Spatial distribution of the acoustic potential in the macroscopic domain.

3.1. Biot model and double porosity

The Biot model involves three essential constitutive laws: 1) the relationship between the drained solid skeleton "macroscopic" deformation $\boldsymbol{e}(t,x)$, the fluid pressure in pores $p(t,x)$ and the total stress $\boldsymbol{\sigma}(t,x)$, 2) the relationship between the variation of the fluid content, skeleton (macroscopic) deformation, and the fluid pressure, 3) the Darcy law relating the seepage velocity, $\boldsymbol{w}(t,x)$, with "dynamic fluid pressure", i.e. the static part $p(t,x)$ and the fluid inertia part. In the DISSERTATION , only quasistatic problems are studied so that the following form of the equations is relevant:

$$\begin{aligned} -\nabla\cdot(\boldsymbol{D}\boldsymbol{e}(\boldsymbol{u})) + \nabla\cdot(\boldsymbol{\alpha}p) &= \boldsymbol{f}\ , \\ \boldsymbol{K}^{-1}\boldsymbol{w} + \nabla p &= 0\ , \\ \boldsymbol{\alpha} : \boldsymbol{e}(\dot{\boldsymbol{u}}) + \nabla\cdot\boldsymbol{w} + \frac{1}{\mu}\dot{p} &= 0\ , \end{aligned} \tag{13}$$

where $\boldsymbol{D}$ is the elasticity tensor associated to the drained skeleton, $\boldsymbol{K}$ is the hydraulic permeability (specific to a given fluid), α is the poroelastic stress coefficient and μ is the Biot modulus which depends on compressibility of the solid skeleton and fluid. Obviously, the three field formulation can be reduced to the two field formulation by eliminating $\boldsymbol{w}$. Further reduction of the model is possible when both the phases are incompressible, i.e. when $1/\mu \to 0$ and $\boldsymbol{\alpha} \to \boldsymbol{I}$.

Double porosity and permeability scaling The double porous media are frequent in nature. Besides various fissured rocks, the dual porosity is presented by the canalicular network of the so-called matrix constituting the structure of cortical bone tissue, see Fig. 5, Rohan et al. (2012).

In the *dual porosity*, the permeability coefficient is proportional to ε^2, where ε is the dimensionless scale parameter. In Fig. 4, the *dual porosity* is represented by an array of"horizontal" channels of the

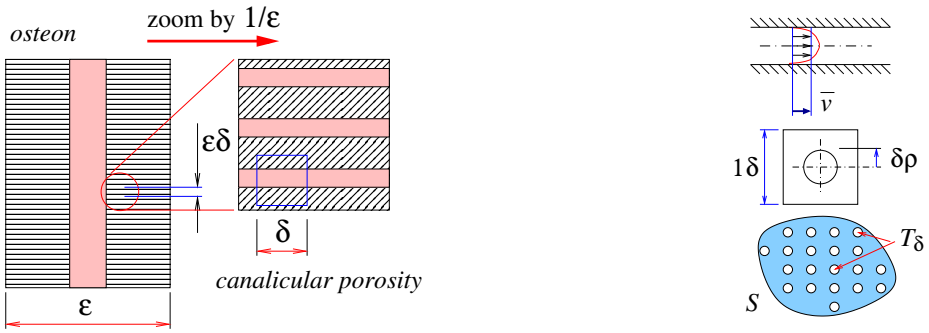

Fig. 4: Left: schematic illustration of the osteon double porous structure. Right: a scheme explaining the permeability δ^2-dependence due to the velocity profile in an array of canals. The total perfused area S is perforated by canals with total cross-section T_δ (bottom), each canal has the cross-section $\pi\rho^2\delta^2$; the square periodic cell is shown (middle) as well as the velocity profile in one canal. (top).

canalicular porosity. It can be shown, Rohan et al. (2012) that if the ratio between the macro-, meso- and micro- scales is the same, i.e. $\delta \sim \varepsilon$, the scale dependent permeability is $\sim \varepsilon^2$, so that the seepage in the dual porosity is given by $\boldsymbol{w}^\varepsilon = -\varepsilon^2 \boldsymbol{K}_\nu \nabla p$, where $\boldsymbol{K}_\nu$ is disproportional to the fluid viscosity.

3.2. Homogenization of FSPM with application in biomechanics

The theory of FSPM has been developed in adherence to applications in civil engineering, oil industry, mining and rock mechanics. Also the tissue biomechanics presents a new challenging field of applications, due to large complexity of processes and interactions undergoing in living tissues.

In contrast with soils, rocks and materials used in civil engineering, the biological materials exhibit much larger organization of their structure. To illustrate the difference, one can consider seepage and consolidation in moist soils, on one hand, and the sophisticated system of heart muscle perfusion, on the other hand. In both these cases, the material contains the solid and liquid phases, however, the structure of pores is very different.

There are several problems in the tissue biomechanics were homogenization with the dual porosity ansatz can be employed as a convenient modelling tool.

- The *smooth muscle tissue* model (Rohan, 2006b) is based on the large deforming FSPM with locally periodic structure. The representative cell contains the fluid-filled inclusion representing the muscle cell. The cytoskeleton is approximated very roughly as a truss with prestretch corresponding to the cell contraction. The extracellular space (the matrix) represents the dual porosity, whereby fluid can flow between the matrix and the cell due permeability of the cell surface. Although from the physiological point of view this model is naive, it contains some important features and can serve as a basis for further model improvements and investigations of the mechanical interactions related to various regimes of tissue contraction.

- The *compact bone* poroelasticity model (Rohan et al., 2012; Rohan and Cimrman, 2011) describes interactions between deformation of the bone tissue and induced flow in the double-porous structure consisting of the Havers-Volkmann channels (the primary porosity) and the canaliculi (the dual porosity). This model is being developed to understand how the flow in the canaliculi populated by mechano-sensitive bone cells depends on the macroscopic load, since this phenomenon influences significantly the bone tissue growth and remodeling.

- The model describing *blood perfusion in deforming tissue* (Rohan, 2006a; Rohan and Cimrman, 2010; Rohan and Lukeš, 2010a) is relevant to the lower levels of the "perfusion tree". The two systems of channels characterize the arterial and venous sectors which exchange the fluid (bood) through the matrix representing the dual porosity. The model has been extended for the large deformation using the linearization based on the updated Lagrangian formulation.

- The model of *blood perfusion in "layered tissues"* (Rohan, 2010) is an attempt to cope with branching organization of the perfusion tree. The tissue periodicity is confined to two directions

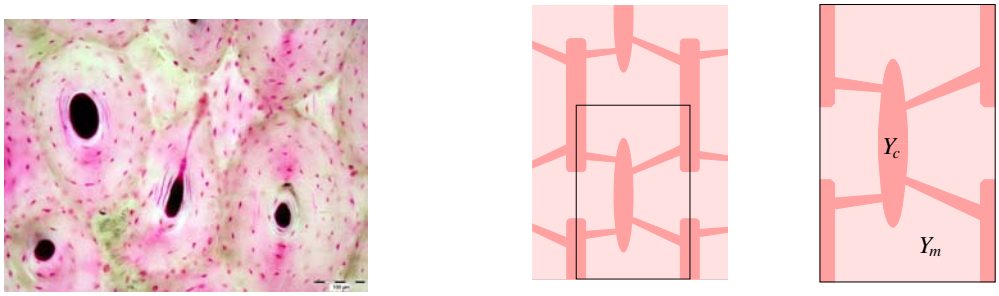

Fig. 5: **Left:** *a micrograph of the osteon porosity arranged in cylindrical geometry. The Haversian canals form the center of each osteon bounded by the cement line. The osteon matrix is penetrated by canalicular porous network arranged almost radially with respect to the osteon axis. (The color image provided by courtesy of Zbyněk Tonar.)* **Right:** *microstructure decomposition w.r.t. the dual porosity: dark pink: Ω_c, light pink: Ω_m, and the representative periodic cell Y decomposition.*

associated with the layer mean-surface, whereas there is no periodicity in the transversal direction. Thus, the tissue volume in 3D can be decomposed into several layers and the homogenization provides several 2D coupled problems, one per each layer.

Two compartment topology of the microstructure The two compartment topology of the microstructure is convenient for modeling bone tissue. Its structure is formed by Haversian and Volkmann channels (the primary porosity) and by porous matrix perforated by canaliculi (the dual porosity).

For finite scale $\varepsilon > 0$ domain $\Omega \subset \mathbb{R}^3$ is decomposed into two principal nonoverlapping parts, the channels Ω_c^ε and the matrix Ω_m^ε, so that $\Omega = \Omega_m^\varepsilon \cup \Omega_c^\varepsilon \cup \Gamma_{mc}^\varepsilon$, $\Gamma_{mc}^\varepsilon = \overline{\Omega_m^\varepsilon} \cap \overline{\Omega_c^\varepsilon}$ is the channel-matrix interface. Domain Ω is generated as a periodic lattice using a representative periodic cell $Y = Y_c \cup Y_m \cup \Gamma$, see Fig. 5 (right), where Y_c generating Ω_c^ε represent the channels of the primary porosity separated from the matrix $Y_m = Y \setminus \overline{Y_c}$ by interface Γ.

The model of the homogenized bone tissue is obtained using the Biot model (13). Following the double-porosity ansatz, the permeability $\boldsymbol{K}^\varepsilon$ is scaled by ε^2 in the dual porosity represented by Y_m, namely using the unfolding operator $\mathcal{T}_\varepsilon(\boldsymbol{K}^\varepsilon(x)) = \varepsilon^2 \chi_m(y)\boldsymbol{K}^m(y) + \chi_c(y)\boldsymbol{K}^c(y)$ with $y \in Y$, $x \in \Omega$, where χ_d, $d = m, c$ is the characteristic function of domain Y_d.

The homogenized equations involve stationary and non-stationary homogenized coefficients which serve as convolution kernels and, thus, are responsible for the fading memory effects. These effects are induced by microflows in the dual porosity, due to the fluid-structure interaction at the microscopic level.

In order to compute the homogenized coefficients, microscopic problems must be solved, so that the characteristic responses of the computational cell Y are obtained, see Fig. 6.

All details upon derivation of the homogenized equations can be found in Rohan et al. (2012). The macroscopic problem can be presented in the weak form: for a.a. $t \in]0, T[$ find couple $(\boldsymbol{u}(t,\cdot), p(t,\cdot)) \in V \times H^1(\Omega)$ ($V \subset \mathbf{H}^1(\Omega)$ is determined by kinematic boundary conditions) with initial condition

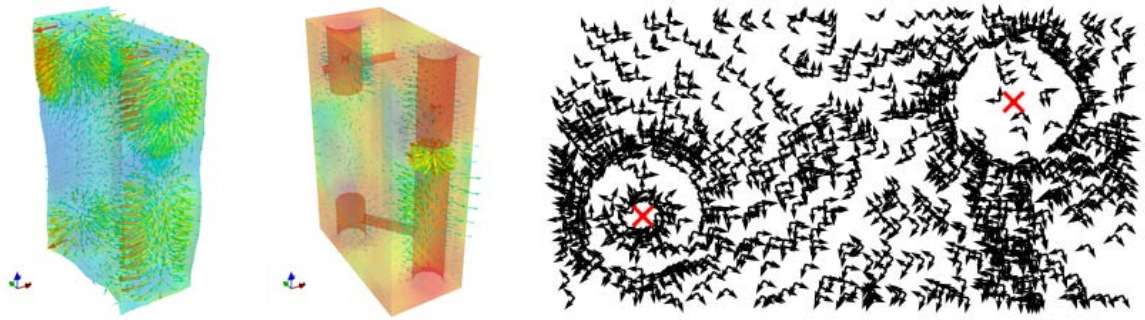

Fig. 6: Characteristic response in the reference cell Y – illustration of corrector basis functions (left) and anisotropy of the permeability in the dual porosity (right).

$p(0,\cdot)=0$, such that

$$\int_\Omega \mathcal{E}_{ijkl}e_{kl}(\boldsymbol{u})e_{ij}(\boldsymbol{v}) + \int_\Omega\int_0^t \mathcal{H}_{ijkl}(t-\tau)e_{kl}(\frac{\mathrm{d}}{\mathrm{d}\,\tau}\boldsymbol{u}(\tau))\,d\tau\, e_{ij}(\boldsymbol{v})$$
$$-\int_\Omega (\mathcal{B}_{ij}+\mathcal{P}_{ij}(0))\,p\,e_{ij}(\boldsymbol{v}) - \int_\Omega\int_0^t \frac{\mathrm{d}}{\mathrm{d}\,t}\mathcal{P}_{ij}(t-\tau)p(\tau)\,d\tau\, e_{ij}(\boldsymbol{v}) = \int_{\partial_\sigma\Omega}\boldsymbol{g}\cdot\boldsymbol{v}\,d\Gamma\ , \tag{14}$$

$$\int_\Omega (\mathcal{B}_{ij}+\mathcal{P}_{ij}(0))\,e_{ij}(\frac{\mathrm{d}}{\mathrm{d}\,t}\boldsymbol{u})\,q + \int_\Omega\int_0^t \frac{\mathrm{d}}{\mathrm{d}\,t}\mathcal{P}_{ij}(t-\tau)e_{ij}(\frac{\mathrm{d}}{\mathrm{d}\,\tau}\boldsymbol{u}(\tau))\,d\tau\,q$$
$$+\int_\Omega \mathcal{C}_{ij}\partial_j p\partial_i q + \int_\Omega q\mathcal{M}\frac{\mathrm{d}}{\mathrm{d}\,t}p + \int_\Omega q\int_0^t \mathcal{N}(t-\tau)\frac{\mathrm{d}}{\mathrm{d}\,\tau}p(\tau)\,d\tau = 0\ ,$$

for all $\boldsymbol{v}\in V_0$ and $q\in H^1(\Omega)$.

Model (14) was implemented numerically, details on the FE discretization and evaluation of the convolution integrals can be found in Rohan and Cimrman (2011).

Three compartment topology In perfused tissues the three compartments correspond to two systems of channels (the arterial and venous sectors) separated by the matrix representing the tissue penetrated by capillaries which form the dual porosity.

In analogy with the two-compartment model, for finite scale $\varepsilon>0$ domain $\Omega\subset\mathbb{R}^3$ is decomposed into three principal nonoverlapping parts, the channels $\Omega^\varepsilon_\alpha$, $\alpha=1,2$ and the matrix Ω^ε_3, so that $\Omega=\bigcup_{i=1,2,3}\Omega^\varepsilon_i\cup\Gamma^\varepsilon_{23}\cup\Gamma^\varepsilon_{13}$, where $\Gamma^\varepsilon_{\alpha 3}$ are the channel-matrix interfaces. The reference cell Y is decomposed accordingly: the channels are represented by Y_1 and Y_2 which are mutually disjoint, i.e. $Y_1\cap Y_2=\emptyset$, being separated by $Y_3=Y\setminus\bigcup_{\alpha=1,2}\overline{Y_\alpha}$. Obviously, domain Ω^ε_3 is connected.

The homogenization procedure (Rohan, 2006a; Rohan and Cimrman, 2010) is applied to the Biot model (13) with the incompressibility constraints, which yields $\boldsymbol{\alpha}=0$ and $1/\mu=0$. By virtue of the double-porosity ansatz, the permeability $\boldsymbol{K}^\varepsilon$ is scaled by ε^2 in the dual porosity represented by Y_3, so that using the unfolding operator $\mathcal{T}_\varepsilon\Big(K^\varepsilon_{ij}(x)\Big)=\varepsilon^2\chi_3(y)K^3_{ij}(y)+\sum_{\alpha=1,2}\chi_\alpha(y)K^\alpha_{ij}(y)$, $y\in Y$, $x\in\Omega$.

As the result of the homogenization, a two-scale system of equations is obtained. Using the Laplace transformation, the two-scale problem is decoupled: *the local microscopic problems* are solved in reference cell Y to obtain the characteristic responses. Consequently, the homogenized coefficients involved in the macroscopic problem can be evaluated using corrector basis functions, see Rohan and Cimrman (2010): quantities.

- $\mathcal{E}_{ijkl}$ is the elasticity tensor. It expresses the overall elasticity (stiffness) of the dried porous skeleton represented by domain Y, thus, including both the porosities.
- $\mathcal{H}_{ijkl}(t)$ is the viscosity tensor related to the macroscopic creep and relaxation phenomena; it expresses the microflow (perfusion) in the dual porosity Y_3.

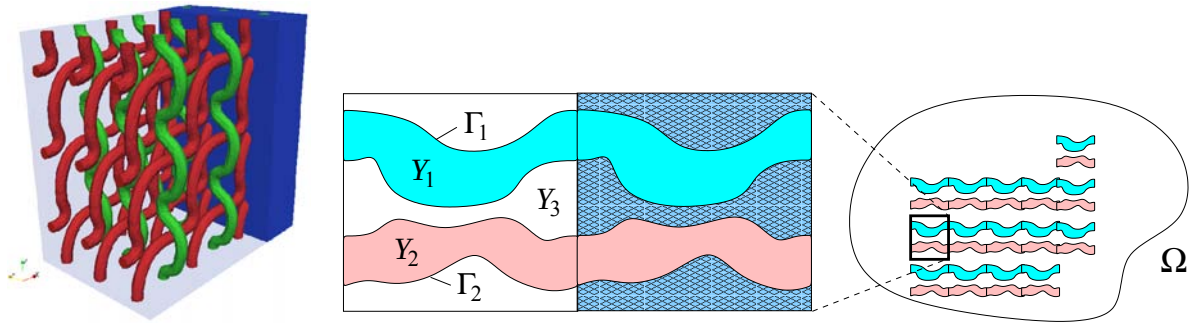

Fig. 7: Left: a three-compartment periodic structure, Right: the scheme of the microstructure decomposition.

- $\mathcal{R}^1_{ij}(t)$ and $\bar{\mathcal{P}}^1_{ij}$ are the poroelastic coefficients which reflect two phenomena: the elasticity of the dried skeleton in Y and permeability of the dual porosity.
- $\tilde{\mathcal{G}}_+(t)$ and $\mathcal{G}^*$ are the perfusion coefficients which control the amount of the fluid exchange between sectors Y_1 and Y_2.
- $\mathcal{C}^\alpha_{ij}$ is the homogenized permeability of the primary porosity in Y_α.

The macroscopic perfusion model describes parallel flows through the two channel systems in deforming medium. The macroscopic displacement field, $\boldsymbol{u}^0(t,\cdot) \in \boldsymbol{V} \subset \mathbf{H}^1(\Omega)$, and the two macroscopic pressures, $p_1(t,\cdot), p_2(t,\cdot) \in H^1_0(\Omega)$ satisfy the equilibrium equation (compare with the two-compartment model (14))

$$\begin{aligned}
&\int_\Omega \left[\mathcal{E}_{ijkl} e^x_{kl}(\boldsymbol{u}^0(t,\cdot)) + \int_0^t \mathcal{H}_{ijkl}(t-\tau)\,\frac{\mathrm{d}}{\mathrm{d}\,\tau} e^x_{kl}(\boldsymbol{u}(\tau,\cdot))\,d\tau\right] e^x_{ij}(\boldsymbol{v}) \\
&- \int_\Omega e^x_{ij}(\boldsymbol{v}) \int_0^t \tilde{\mathcal{R}}^1_{ij}(t-\tau)[p_1(\tau,\cdot) - p_2(\tau,\cdot)]\,d\tau \\
&- \sum_{\alpha=1,2} \int_\Omega \left[\frac{|Y_\alpha|}{|Y|}\delta_{ij} + \bar{\mathcal{P}}^\alpha_{ij}\right] p_\alpha(t,\cdot)\, e^x_{ij}(\boldsymbol{v}) = \int_{\partial_\sigma\Omega} \boldsymbol{g}\cdot\boldsymbol{v}\,dS \quad \forall \boldsymbol{v} \in \boldsymbol{V}_0\ ,
\end{aligned} \tag{15}$$

and the two balance-of-mass equations for $\alpha, \beta = 1, 2,\ \beta \neq \alpha$

$$\begin{aligned}
&\int_\Omega \mathcal{C}^\alpha_{ij}\,\partial^x_j p_\alpha(t,\cdot)\,\partial^x_i q + \int_\Omega q\,\mathcal{G}^*\frac{\mathrm{d}}{\mathrm{d}\,t}\left(p_\alpha(t,\cdot) - p_\beta(t,\cdot)\right) \\
&+ \int_\Omega q \int_0^t \tilde{\mathcal{G}}_+(t-\tau)\frac{\mathrm{d}}{\mathrm{d}\,\tau}\left(p_\alpha(\tau,\cdot) - p_\beta(\tau,\cdot)\right)\,d\tau \\
&+ \int_\Omega q \int_0^t \tilde{\mathcal{R}}^\alpha_{ij}(t-\tau)\frac{\mathrm{d}}{\mathrm{d}\,\tau} e^x_{ij}(\boldsymbol{u}^0(\tau,\cdot))\,d\tau \\
&+ \int_\Omega q \left[\frac{|Y_\alpha|}{|Y|}\delta_{ij} + \bar{\mathcal{P}}^\alpha_{ij}\right]\frac{\mathrm{d}}{\mathrm{d}\,t} e^x_{ij}(\boldsymbol{u}^0(t,\cdot)) = 0\ , \quad \forall q \in H^1_0(\Omega)\ ,
\end{aligned} \tag{16}$$

which govern the fluid flows in the two channels and its redistribution between them. The terms involving the pressure difference $p_\alpha - p_\beta$ reveal the amount of perfused fluid; while coefficient $\mathcal{G}^*$ is related to transition effects, the perfusion in a steady state is determined by the convolution term involving $\tilde{\mathcal{G}}_+(t-\tau)$, since $\tilde{\mathcal{G}}_+(+\infty) > 0$.

The three-compartment two-scale model was implemented in the **SfePy** FE code (Cimrman and et al., 2011). As an example, in Fig. 8 the pressure and perfusion velocities are displayed for a deforming block of tissue with microstructure similar to that of Fig. 7, right.

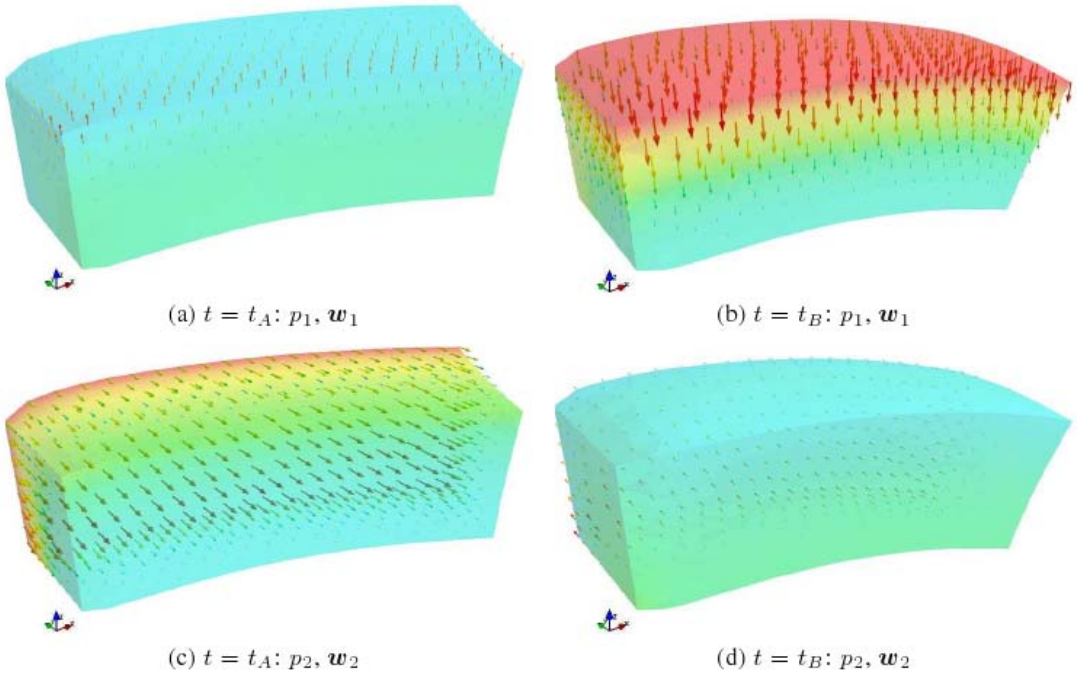

Fig. 8: Deformed perfused block: macroscopic pressures p_1 and p_2 displayed by color map at time $t_A = 60$ s, (a), (c) and $t_B = 80$ s, (b), (d), the associated perfusion velocities are indicated by arrows. Deformation enlarged for visualization. (Computed by R. Cimrman, 2009)

3.3. Homogenization of perfusion in thin layers

Homogenization can be adapted also for structures where the periodicity is restricted to directions within a given plane, as pointed out in Section 2.2..

In paper Rohan (2010) we derived a homogenized model of the Darcy flow in a thin porous non-deformable layer comprising 3 compartments. The reference periodic cell is composed of the matrix representing the dual porosity and of two mutually disconnected channels representing the primary porosity. The resulting model describes macroscopic redistribution of the fluid in the plane to which the thin layer is reduced. Due to the 3D-to-2D reduction and the two-scale decomposition it leads to computationally feasible problem which is now implemented in our in-house developed code *Sfepy*, Cimrman and et al. (2011).

One of the promising applications of the model is the blood perfusion in the brain tissue, see Fig. 9 (left). Although a detailed morphological study is not completed yet, the following assumptions, however simplifying, seem to be relevant:

- change of the microstructure with the depth in the tissue (the radial direction), as indicated by two layers,
- repeated patterns of the microstructure with respect to the tangential direction, so that the periodic "artificial" lattice can be introduced.

Difficulties in modeling the blood perfusion are inherited form the structure of the vascular system which forms vascular trees. An "ideal perfusion tree" can be decomposed into several levels (hierarchies) which can be associated with layers (generated by curved "mean" surfaces); in each of them the vascular network can be approximated by a (locally) periodic structures, where the "plane periodicity" is related to the tangent planes of the generating surface. This simplified view of the real complex system give rise to the idea of decomposing a 3D volume into N layers with a given periodic structure, see Fig. 9 (right), so that the homogenization procedure can be applied.

Problem formulation Homogenization of the Darcy flow in a heterogeneous layer with double porosity was described in Rohan (2010). In Fig. 9 (right) the layer is depicted schematically: Layer $\Omega^\delta =$

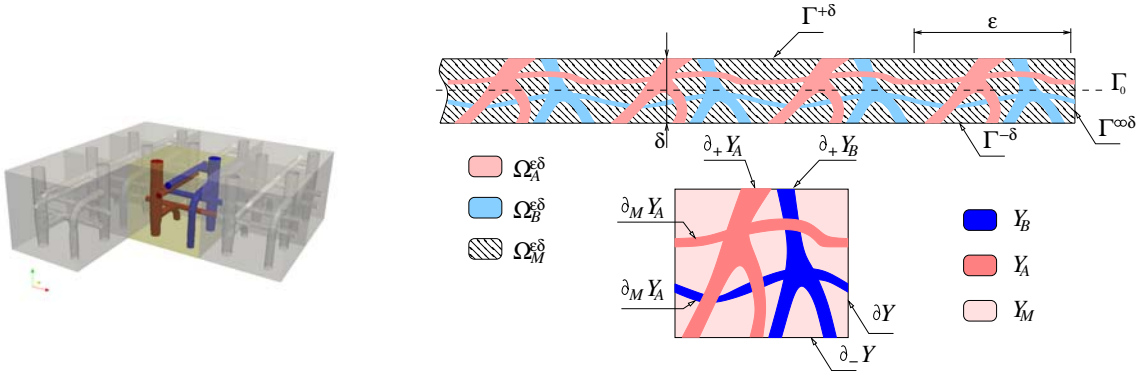

Fig. 9: Left: Representative periodic cell of the layer containing two systems channels. Right: The three compartment heterogeneous layer and the domain and boundary decomposition of the reference periodic cell Y.

$\Gamma_0\times]-\delta/2,+\delta/2[$ has thickness $\delta>0$, whereby $\Gamma_0\subset\mathbb{R}^2$ forms the mean surface. On the "upper" and "lower" boundaries $\Gamma^{\delta+}$ and $\Gamma^{\delta-}$, the fluid exchange with the outer space is controlled by Neumann conditions defined in terms of fluxes $g^{\varepsilon\pm}\in L^2(\Gamma^{\pm})$. Domain Ω^δ consists of three disjoint sectors, the matrix $\Omega_M^{\varepsilon\delta}$ and the two channels $\Omega_A^{\varepsilon\delta}$, $\Omega_B^{\varepsilon\delta}$, which are generated as periodic lattices (with period ε). The double porosity in the matrix $\Omega_M^{\varepsilon\delta}$ is introduced using the standard scaling ansatz for the permeability, as described in preceding sections.

In order to obtain a limit (homogenized) problem, the perfusion fluxes $g^{\pm\varepsilon}$ must be scaled properly with respect to ε: we assume that the fluxes through the matrix interface $\Gamma_M^{\pm\varepsilon}$ are of the order ε, whereas fluxes of the channel inlets and outlets are of the order 1. Moreover, local net sources of channels A and B must be specified. For this we introduce $G_D^\varepsilon(x')$, $x'\in\Gamma_0$, with $D=A,B$, to describe the fluid volume increase per one period ε in the channel compartment D, and assume $G_D^\varepsilon\sim\varepsilon$, i.e. the local source produced in the channel A, or B due to external inlets/outlets is proportional to the thickness $\delta=h\varepsilon$ of the layer.

3.4. Macroscopic equation for single layer

The homogenized problem for pressures p^A and p^B, associated with the channels A and B, describes 2D parallel flows, in homogenized layer $\Gamma_0\subset\mathbb{R}^2$. Each channel system forms a connected domain (so, we assume at least a small co-lateralization of vessels in the perfusion tree). Two coupled "macroscopic" equations (one for A and one for B) involve the homogenized coefficients: permeabilities $(\mathcal{K}_{\alpha\beta})^{A,B}$ of the channels, the transmission $\mathcal{G}$ and drainage $(\mathcal{S}_\alpha)^{A,B,k}$ (for channel branches $k\in J_D$) coefficients. They govern the fluid redistribution between the two channel systems A and B: for A we have the following equation which is coupled with the similar equation for channel B (i.e. the role of indices A and B is exchanged):

$$-\frac{\partial}{\partial x_\alpha}\left[\mathcal{K}^A_{\alpha\beta}\frac{\partial}{\partial x_\beta}p^A+\sum_{k\in J_A}\mathcal{S}^{A,k}_\alpha\tilde{g}^k_A\right]+\mathcal{G}\left(p^A-p^B\right)=c_{hA}\bar{G}_A-\mathcal{F}^{A+}\hat{g}^+-\mathcal{F}^{A-}\hat{g}^-\ ,$$

where $\mathcal{F}^{A+/-}$, c_{hA} are constants (the summation w.r.t. repeated indices α,β applies). Fluxes $\hat{g}^{+/-},\bar{G}_D$ and $\tilde{g}^k_D$, $k\in J_D$, $D=A,B$ are given, such that the solvability conditions hold. The term $\mathcal{G}\left(p^A-p^B\right)$, evaluated at point $x\in\Gamma_0$, expresses the amount of fluid (blood) perfused through the matrix (the dual porosity) between sectors A and B. The details are reported in Rohan (2010).

3.5. Model of N-coupled layers

We consider N layers; in each the perfusion is described by the homogenized model involving macroscopic pressures. Flows between the layers are respected by coupling conditions. In the simplest case, we assume perfect-matching microscopic cells of two attached layers, so that, at the microscopic level, the pressures at the "channel junctions" must equal and the fluxes must be opposite. Analogous conditions

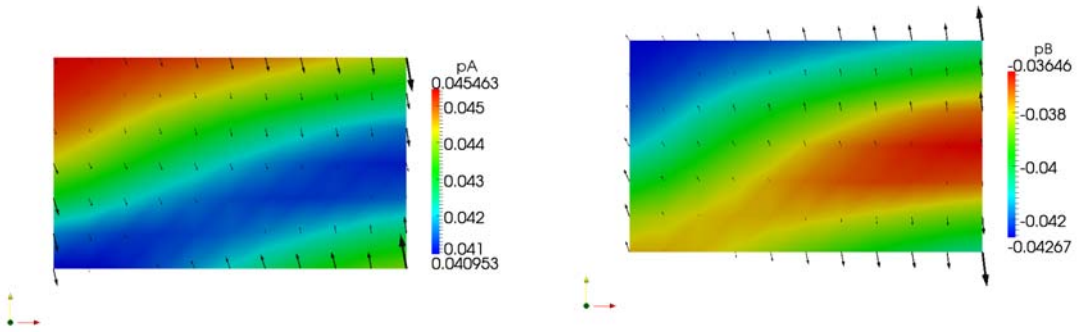

p^A, flux $-\mathcal{K}^A \cdot \nabla p^A$ p^B, flux $-\mathcal{K}^B \cdot \nabla p^B$

Fig. 10: Solutions of the macroscopic problem: macroscopic pressures and fluxes in Γ_0.

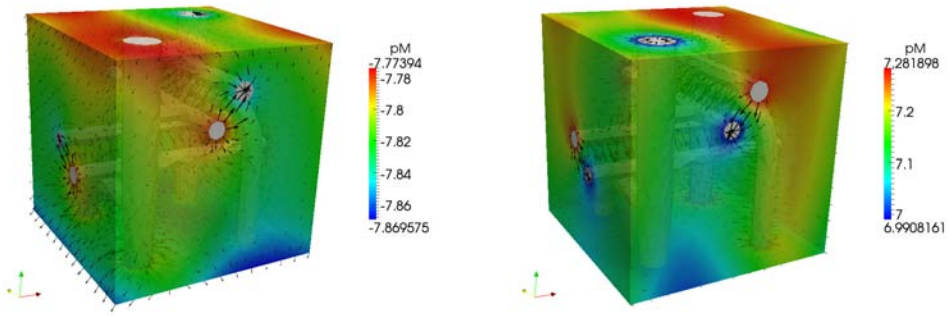

element 1 element 200

Fig. 11: Perfusion reconstruction at the microscopic level — pressure $p_M(x', \cdot)$ *and perfusion velocities* $\boldsymbol{w}_M(x', \cdot)$ *in matrix, as evaluated at two different macroscopic points (elements).*

express coupling for the pressures and fluxes at the interface in the dual porosity. This approach allows us to approximate the hierarchical structure of the perfusion tree: in each layer the periodic microstructure can be different.

Numerical illustration The homogenized single layer model is implemented in code **SfePy** , material coefficients involved in (3.4.) are evaluated for the microstructure of the 3D periodic cell including two channels, see Fig. 9, left. The macroscopic problem is solved for given external fluxes: two "macroscopic" pressures p^A, p^B in Γ_0 are illustrated in Fig. 10, whereby the local amount of the perfused fluid is given by $\mathcal{G}(p^A - p^B)$. Once the macroscopic pressures are computed, at any point of Γ_0, the fluid pressures and perfusion fluxes can be reconstructed at the microscopic level, see an illustration in Fig. 11.

4. Conclusion

The purpose of the paper was to show various applications of the modelling approach based on homogenization of locally periodic structures with strong heterogeneities. The upscaling procedure consists in asymptotic analysis of partial differential equations (PDE) with oscillating coefficients. The strong heterogeneities are represented by scale-dependent coefficients, like elasticity in modelling the phononic materials, or permeability in modelling fluid saturated double porous media. From the mathematical point of view, sequencies of problems parameterized by the heterogeneity scale ε are considered and their limit solutions for $\varepsilon \to 0$ are to be computed. In linear problems, as considered here, the limit model de-

scribing behaviour of the homogenized medium is represented by macroscopic equations which involve constant material coefficients; these can be computed independently of the macroscopic response using characteristic local (microscopic) responses – solutions of autonomous PDEs defined at microscopic level.

The homogenization approach provides computationally efficient schemes for the multi-scale modeling. Once the macroscopic response is obtained, the "microscopic" responses can be reconstructed using the characteristic local responses. There is a remarkable difference with respect to the standard homogenization in using such schemes: while in a standard case the homogenization result is really independent of the heterogeneity scale, in the "large contrast" case the real material coefficients are defined for a given scale $\varepsilon_0 > 0$. This means that the limit model must be interpreted by an extrapolation for the scale $\varepsilon > 0$; for this so-called corrector result is used.

There are many important issues closely related to the topic discussed in this paper. An extension of the homogenization approach for nonlinear problems is cumbersome; apart of the nonlinear techniques based on the Γ-convergence we proposed a linearization approach based on an incremental formulation and an updating scheme for locally periodic microstructures. Another issue of interest is presented by the multi-level (i.e. reiterated) homogenization which allows for modelling heterogeneities at different scales.

Acknowledgments

The research is supported by projects GACR 106/09/0740 and GACR P101/12/2315 of the Czech Scientific Foundation and in a part by the European Regional Development Fund (ERDF), project "NTIS - New Technologies for Information Society", European Centre of Excellence, CZ.1.05/1.1.00/02.0090.

References

Arbogast, T., Douglas, J., and Hornung, U. (1990). Derivation of the double porosity model of single phase flow via homogenization theory. *SIAM J. Math. Anal.*, 21:823–836.

Auriault, J.-L. and Boutin, C. (1992). Deformable porous media with double porosity. quasi statics. i. coupling effects. *Transp. Porous Media*, 7(1):63–82.

Ávila, A., Griso, G., Miara, B., and Rohan, E. (2008). Multiscale modeling of elastic waves: Theoretical justification and numerical simulation of band gaps. *Multiscale Modeling & Simulation, SIAM*, 7:1–21.

Biot, M. A. (1955). Theory of elasticity and consolidation for a porous anisotropic solid. *J. Appl. Phys.*, 26(2):182–185.

Cimrman, R. and et al. (2011). SfePy home page. http://sfepy.org. Software, finite element code and applications.

Cimrman, R. and Rohan, E. (2010). On acoustic band gaps in homogenized piezoelectric phononic materials. *Appl. Comp. Mech.*, 4:89–100.

Cioranescu, D., Damlamian, A., and Griso, G. (2008a). The periodic unfolding method in homogenization. *SIAM Journal on Mathematical Analysis*, 40(4):1585–1620.

Cioranescu, D., Damlamian, A., Griso, G., and Onofrei, D. (2008b). The periodic unfolding method for perforated domains and neumann sieve models. *J. Math. Pures Appl.*, 89:248–277.

Coussy, O. (2004). *Poromechanics*. John Wiley & Sons.

de Boer, R. (2000). *Theory of Porous Media*. Springer, Berlin.

Leugering, G., Rohan, E., and Seifrt, F. (2010). Modeling of metamaterials in wave propagation. In *Wave Propagation in Periodic Media Analysis, Numerical Techniques and practical Applications*. Matthias Ehrhardt (ed.), E-Book Series Progress in Computational Physics,.

Mielke, A. and Rohan, E. (2012). Homogenization of elastic waves in fluid-saturated porous media using the biot model. *Submitted*.

Rohan, E. (2006a). Homogenization approach to the multi-compartment model of perfusion. *PAMM*, 6:79–82.

Rohan, E. (2006b). Modelling large deformation induced microflow in soft biological tissues. *Theor. and Comp. Fluid Dynamics*, 20:251–276.

Rohan, E. (2010). Homogenization of the darcy flow in a double-porous layer. *SIAM, MMS*. Submitted.

Rohan, E. and Cimrman, R. (2010). Two-scale modelling of tissue perfusion problem using homogenization of dual prous media. *Int. Jour. for Multiscale Comput. Engrg.*, 8:81–102.

Rohan, E. and Cimrman, R. (2011). Multiscale FE simulation of diffusion-deformation processes in homogenized dual-porous media. *Math. Comp. Simul.* In Press.

Rohan, E. and Lukeš, V. (2010a). Homogenization of perfusion in large-deforming medium using the updated lagrangian formulation. In *Proceedings of the ECT 2010 conference*. Coburg-Sax Publ.

Rohan, E. and Lukeš, V. (2010b). Homogenization of the acoustic transmission through perforated layer. *J. of Comput. and Appl. Math.*, 6:1876–1885.

Rohan, E. and Miara, B. (2006a). Homogenization and shape sensitivity of microstructures for design of piezoelectric bio-materials. *Mechanics of Advanced Materials and Structures*, 13:473–485.

Rohan, E. and Miara, B. (2006b). Sensitivity analysis of acoustic wave propagation in strongly heterogeneous piezoelectric composite. In *Topics on Mathematics for Smart Systems*, pages 139–207. World Sci. Publishing Company.

Rohan, E. and Miara, B. (2009). Shape sensitivity analysis for material optimization of homogenized piezophononic materials. In *8th World Congress on Structural and Multidisciplinary Optimization*. ECCOMAS.

Rohan, E. and Miara, B. (2011). Band gaps and vibration of strongly heterogeneous reissner-mindlin elastic plates. *Comptes Rendus Mathematique*, 349:777–781.

Rohan, E., Miara, B., and Seifrt, F. (2009). Numerical simulation of acoustic band gaps in homogenized elastic composites. *International Journal of Engineering Science*, 47:573–594.

Rohan, E., Naili, S., Cimrman, R., and Lemaire, T. (2012). Multiscale modelling of a fluid saturated medium with double porosity: Relevance to the compact bone. *Jour. Mech. Phys. Solids*, 60:857–881.

Sanchez-Palencia, E. (1980). *Non-homogeneous media and vibration theory*. Number 127 in Lecture Notes in Physics. Springer, Berlin.